ISBN: 978-3-95450-223-3 ISSN: 2673-7000 doi:10.18429/JACoW-NAPAC2019-WEPLS05

SIMULATION ANALYSIS OF THE LCLS-II INJECTOR USING ACE3P AND IMPACT

D. Bizzozero, J. Qiang, Lawrence Berkeley National Laboratory, Berkeley, CA, USA
L. Ge, Z. Li, C-K Ng, L. Xiao, SLAC National Accelerator Laboratory, Menlo Park, CA, USA

Abstract

The LCLS-II beam injector system consists of a 186 MHz normal-conducting RF gun, a two-cell 1.3 GHz normal-conducting buncher cavity, two transverse focusing solenoids, and eight 1.3 GHz 9-cell Tesla-like superconducting booster cavities. With a coordinated effort between SLAC and LBNL, we have developed a simulation workflow combining the electromagnetic field solvers from ACE3P with the beam dynamics modeling code IMPACT. This workflow will be used to improve performance and minimize beam emittance for given accelerator structures through iterative optimization. In our current study, we use this workflow to compare beam quality parameters between using 2D axisymmetric field profiles and fully 3D non-axisymmetric fields caused by geometrical asymmetries (e.g. RF coupler ports).

OVERVIEW OF ACE3P AND IMPACT

We begin with a brief description of the simulation tools used in our study. The ACE3P code suite [1], developed at SLAC, consists of several tools for various types electromagnetic problems. One such tool, the code Omega3P [2], is a complex eigenmode solver for finding normal modes in RF structures. By using Omega3P with physical design geometries for beamline components, we can export electromagnetic field maps in regions of interest.

Next, the IMPACT code [3–5], developed at LBNL, consists of two particle tracking solvers IMPACT-T (time-coordinate-based) and IMPACT-Z (z-coordinate-based). For our study, we use the IMPACT-T solver to self-consistently track a particle bunch as it propagates through an injector lattice defined by various accelerator structures.

For the analysis in this paper, we use Omega3P to generate high-resolution 3D electric and magnetic field maps for several accelerator components and import them into IMPACT-T for particle tracking as an external field.

In a current configuration, we have implemented a Python script to encapsulate the ACE3P-IMPACT simulation process in a single routine. This script reads-in geometry mesh files, runs Omega3P to compute eigenmodes in various RF cavities, exports the fields into an openPMD hierarchical data structure [6], and runs IMPACT-T on the desired lattice design. In the future, this script will be used as part of a beam optimizer in which the ACE3P-IMPACT workflow is framed as an objective function and optimized by adjusting the geometry and other parameters in an iterative scheme.

PROPOSED LCLS-II INJECTOR DESIGN

In this section, we overview the LCLS-II injector beamline lattice used in our simulation. This design beamline begins with a 186 MHz normal-conducting RF gun, followed by a focusing solenoid, a two-cell 1.3 GHz normal-conducting buncher cavity, a second focusing solenoid, and eight 9-cell 1.3 GHz superconducting boosting cavities for a total length of 14 m, see Figure 1.

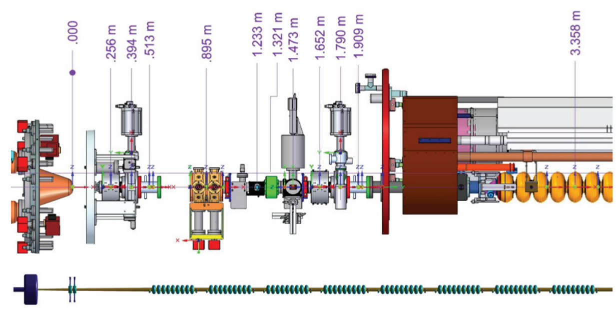

Figure 1: (Top) Schematic layout of the first 3.5 m of the proposed LCLS-II injector (image courtesy of LCLS-II). (Bottom) Full 14 m diagram of the LCLS-II injector RF model (focusing solenoids not shown).

For the beam parameters used in our study, we assume an initial uniform cylindrical electron bunch with charge 100–300 pC, length 34 μm, and radius 0.64 mm. The initial momentum distribution is taken as the product of a zero-mean transverse Gaussian profile with $\sigma_{px,py} = 1.0 \times 10^{-3} m_e c$ and a longitudinal shifted semi-Gaussian profile given by:

$$\rho_{pz}(p_z) = \frac{p_z - p_{z,\min}}{\sigma_{pz}^2} \exp\left[-(p_z - p_{z,\min})^2/(2\sigma_{pz}^2)\right], \quad (1)$$

for $p_z > p_{z,\min} = 2.0 \times 10^{-3} m_e c$ and $\sigma_{pz} = 1.0 \times 10^{-3} m_e c$. This longitudinal distribution ensures all particles have an initial momentum of at least $p_{z,\min}$ for use in simulations.

One important aspect for the LCLS-II injector lattice is to consider the effects of ports and couplers on quantities of interest such as beam emittance. We aim to closely analyze the emittance growth due to the couplers in the boosting cavities through theoretical considerations and numerical simulations.

EMITTANCE GROWTH ESTIMATES

As a reference point for our simulations, we refer to earlier work by Dowell et al [7], which derives an approach to estimate the transverse emittance growth due to the asymmetric couplers. In that study, the couplers in an entire boosting

ISBN: 978-3-95450-223-3 ISSN: 2673-7000 doi:10.18429/JACoW-NAPAC2019-WEPLS05

cavity are modeled by an instantaneous momentum kick to the particles.

To briefly overview their result, the authors compute the complex voltage kick factor for the booster cavity:

$$\vec{V}(x,y) = \int \left[\vec{E}(x,y,z) + ic\vec{\beta} \times \vec{B}(x,y,z)\right] e^{2\pi i f z/c} dz, \tag{2}$$

where $f = 1.3$ GHz is the RF cavity phase and $\beta \approx 1$. Next, by normalizing $\vec{V}$ by the on-axis longitudinal kick $V_z(0,0)$, they define $\vec{v}(x,y) := \vec{V}(x,y)/V_z(0,0)$. Lastly, by linearizing the quantity $\vec{v}(x,y) = [v_x(x,y), v_y(x,y), v_z(x,y)]$ about $(0,0)$ they obtain an expression for the cross terms:

$$v_{xy} = \left.\frac{\partial v_x}{\partial y}\right|_{(x,y)=(0,0)}, \quad v_{yx} = \left.\frac{\partial v_y}{\partial x}\right|_{(x,y)=(0,0)}. \tag{3}$$

After a lengthy derivation with several assumptions, the authors arrive at a convenient estimation formula for the normalized emittance growth of a thin bunch from a coupler:

$$\Delta\epsilon_{x,y} = \frac{eV_{\text{acc}}}{m_e c^2}\sigma_{x,y}^2 \left|\text{Re}(v_{xy})\cos\phi + \text{Im}(v_{xy})\sin\phi\right|, \tag{4}$$

where ϕ is the bunch phase with respect to the RF field (in our case $\phi \approx 0$), and v_{xy} is defined as in Eq. (3). Lastly, assuming $\vec{E}$ and $\vec{B}$ vary linearly transversely on the scale of the bunch size, the cross terms satisfy $v_{xy} = v_{yx}$.

Equation (4) assumes no momentum spread or correlation such that $\langle x^2\rangle = \sigma_x^2$ and $\langle y^2\rangle = \sigma_y^2$ are the only nonzero terms in the 4×4 matrix describing a phase-space ellipse in (x, y, x', y'). More details can be found in [7].

SIMULATIONS AND RESULTS

As discussed in the code overview section, we use Omega3P to accurately compute the field eigenmodes for the RF gun, bunching cavity, and boosting cavities. With the full cavity eigenmode solutions, we crop the field data around small box-shaped region containing the particle trajectory and convert the format using the openPMD standard formatting to be read-in by IMPACT.

We now use IMPACT to generate a 300 pC electron bunch modeled by 10^6 macroparticles with the 6D phase space distribution as prescribed in the LCLS-II injector design section. The bunch is tracked from the electron emission process until after exiting the final boosting cavity, approximately 14 m in total length.

In the IMPACT code, the three RF cavity types: photo RF gun, buncher, and booster, are loaded as external electromagnetic fields and scaled with different peak fields. Table 1 lists the components used in the LCLS-II injector simulation. Boosting cavities 2 and 3 are set to "off" with no applied voltage. The lengths shown include short symmetric drift tubes on either end of the cavity and offset position is defined as distance from the nearest tube edge to the photocathode.

To investigate the effects on beam emittance induced by the RF power couplers in the boosting cavities, we performed

Table 1: LCLS-II Simulation Lattice Components

Component	Length	Offset	Peak field
Photo RF Gun	0.200 m	0.000 m	20.0 MV/m
Solenoid 1	0.016 m	0.480 m	57.2 mA/m
Buncher	0.358 m	0.630 m	2.12 MV/m
Solenoid 2	0.016 m	1.411 m	35.2 mA/m
Booster 1	1.348 m	2.670 m	15.4 MV/m
Booster 2	1.348 m	4.054 m	0.00 MV/m
Booster 3	1.348 m	5.437 m	0.00 MV/m
Booster 4	1.348 m	6.821 m	30.0 MV/m
Booster 5	1.348 m	8.204 m	32.0 MV/m
Booster 6	1.348 m	9.588 m	32.0 MV/m
Booster 7	1.348 m	10.972 m	32.0 MV/m
Booster 8	1.348 m	12.355 m	32.0 MV/m

two simulations. To remove any coupler-induced emittance, we constructed an axisymmetric boosting cavity model and compared it with a model using full geometry including couplers. Aside from the boosting cavity fields, both simulations used identical beam and lattice parameters.

The particle energy plot is shown in Figure 2. We note that the first boosting cavity produces an acceleration voltage $V_{\text{acc}} = 8.1$ MV and the final particle energy after the injector is approximately 94 MeV.

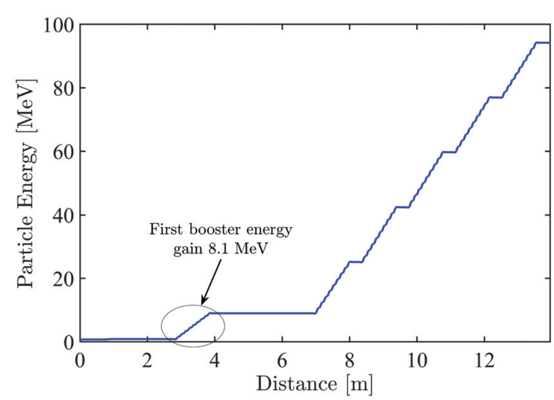

Figure 2: Mean particle energy vs distance along the injector. The acceleration voltage V_{acc} for the first booster is 8.1 MV.

Next, the RMS transverse bunch size in the injector extends to almost 5 mm as shown in Figure 3. The bunch radius inside the first boosting cavity varies in the range of $\sigma_{x,y} = 1.5-3.5$ mm with a mean value of $\bar{\sigma}_{x,y} = 2.2$ mm.

Lastly, for an emittance growth estimation using (4), we computed $v_{xy} = (4.8 + 1.3i) \times 10^{-3}\ \text{m}^{-1}$ from the eigenmode field data of the first boosting cavity computed using Omega3P and the component parameters given in Table 1. Using Eq. (4) with the parameters for the first boosting cavity, we estimate the emittance growth due to the couplers after the first boosting cavity to be $\Delta\epsilon_{x,y} \approx 0.35$ mm mrad.

When examining the RMS normalized transverse emittance from our simulations, we note an emittance difference between the axisymmetric and full geometry models after first boosting cavity as shown in Figure 4 (top). The

ISBN: 978-3-95450-223-3 ISSN: 2673-7000 doi:10.18429/JACoW-NAPAC2019-WEPLS05

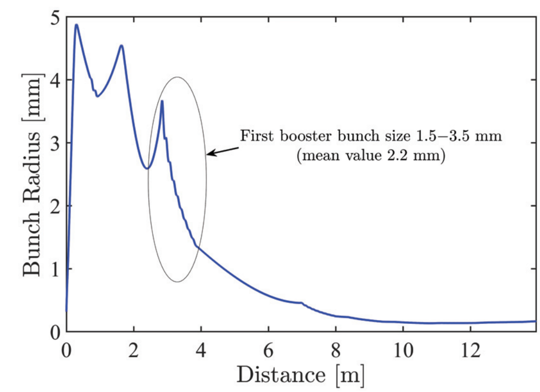

Figure 3: Bunch radius (RMS) vs distance along the injector. The transverse bunch size compresses from 3.5 mm to 1.5 mm in the first boosting cavity.

emittance difference at the end of the injector is $\Delta\epsilon_{x,y}$ = 0.15 mm mrad or approximately 11% as seen in Figure 4. The relative difference between the two simulations decays to approximately 7% by the end of the injector as shown in Figure 4 (bottom).

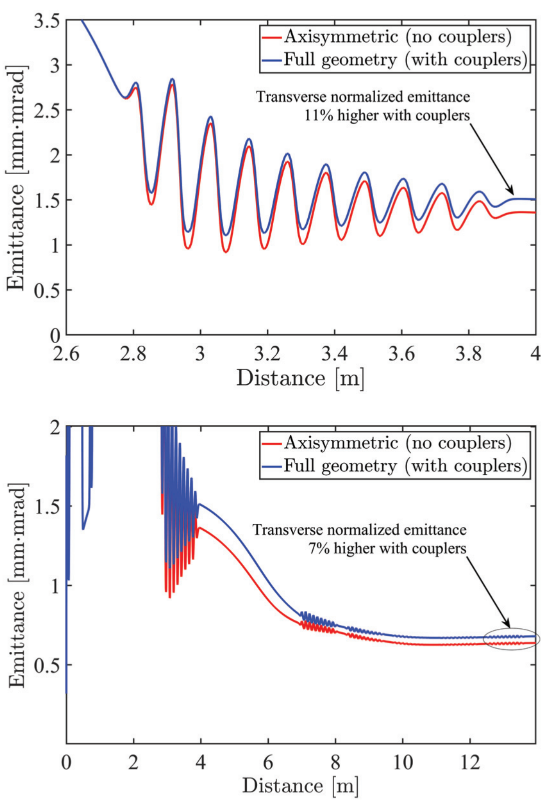

Figure 4: Transverse normalized emittance comparison between models inside the first booster (top) and the entire injector (bottom).

CONCLUSIONS

We have successfully integrated ACE3P and IMPACT into a single workflow routine using the Python programming language. The workflow currently consists of: the Omega3P code, an openPMD conversion tool, and the IMPACT-T code. Future developments will include an output post-processing routine, a parameter optimizer, and an automated model and mesh generator. These additional tools in the workflow will enable coupled beam and/or geometry parameter optimization using an iterative scheme.

For our current benchmark, we have tested the workflow for a proposed set of parameters for the LCLS-II injector. Our numerical simulations using Omega3P and IMPACT-T conclude that while there is an increase in transverse emittance due to the presence of couplers in the boosting cavities, this increase is less than predicted by earlier studies [7, 8].

Since the emittance growth from couplers are sensitive to the transverse size $\sigma_{x,y}$ as shown in Eq. (4), it is possible that the emittance may be higher or lower than predicted by our simulation if the initial bunch distribution is slightly different.

With regards to the injector design, if the emittance from couplers increases beyond a desired limit, the addition of quadruples in the lattice can offset this increase as implemented at various accelerator facilities [9, 10].

ACKNOWLEDGMENTS

This work is supported by the Director of the Office of Science of the US Department of Energy under contracts DE-AC02-05-CH11231 and DE-AC02-76-SF00515.

REFERENCES

[1] ACE3P (Advanced Computational Electromagnetics 3P) Code Suite, https://portal.slac.stanford.edu/sites/ard_public/acd/Pages

[2] L.-Q. Lee, "A Parallel Finite-Element Eigenmode Analysis Code for Accelerator Cavities," SLAC Technical Report, SLAC-PUB-13529, 2009.

[3] J. Qiang, R. Ryne, S. Habib, and V. Decyk, "An Object-Oriented Particle-In-Cell Code for Beam Dynamics Simulation in Linear Accelerators," *J. Comp. Phys.*, vol. 163, p. 434, 2000.

[4] J. Qiang, S. Lidia, R. Ryne, and C. Limborg-Deprey, "Three-dimensional quasistatic model for high brightness bream dynamics simulation," *Phys. Rev. ST Accel. Beams*, vol. 9, p. 044204, 2006.

[5] J. Qiang *et al.*, "High resolution simulation of beam dynamics in electron linacs for x-ray free electron lasers," *Phys. Rev. ST Accel. Beams*, vol. 12, p. 100702, 2009.

[6] A. Huebl *et al.*, "openPMD: A meta data standard for particle and mesh based data, technical specification (CC-BY 4.0)," November 2015. doi:10.5281/zenodo.591699

[7] D. H. Dowell, F. Zhou, and J. Schmerge, "Exact cancellation of emittance growth due to coupled transverse dynamics in solenoids and rf couplers," *Phys. Rev. Accel. Beams*, vol. 21, p. 010101, 2018.

ISBN: 978-3-95450-223-3 ISSN: 2673-7000 doi:10.18429/JACoW-NAPAC2019-WEPLS05

[8] A. Vivoli *et al.*, "Effect of Cavity Couplers Field on the Beam Dynamics of the LCLS-II Injector", in *Proc. 27th Linear Accelerator Conf. (LINAC'14)*, Geneva, Switzerland, Aug.-Sep. 2014, paper THPP060, pp. 989–991.

[9] T. Schietinger *et al.*, "Commissioning experience and beam physics measurements at the SwissFEL Injector Test Facility," *Phys. Rev. Accel. Beams*, vol. 19, p. 100702, 2016.

[10] A. Bartnik *et al.*, "Operational experience with nanocoulomb bunch charges in the Cornell photoinjector," *Phys. Rev. Accel. Beams*, vol. 18, p. 083401, 2015.